1,3-Diethynyl-5-(X)-benzene-Bridged [Cp*(dppe)Fe]n+ Units: Effect of Substituents on the Metal-Metal Interactions

J. Lepont, Thierry Roisnel, Jean-René Hamon, C. Lapinte

10.1002/ejic.202100789

1,3-Diethynyl-5-(X)-benzene-Bridged [Cp*(dppe)Fe]$^{n+}$ Units: Effect of Substituents on the Metal-Metal Interactions

Joseph Lepont,[a] Thierry Roisnel,[a] Jean-René Hamon,*[a] and Claude Lapinte*[a]

Dedicated to our distinguished colleague Dr Christian Bruneau who enriched organometallic and catalysis communities with his numerous scientific achievements and amiable personality.

Abstract: The new complexes [1,3-{Cp*(dppe)Fe-C≡C-}$_2$-5-(X)-(C_6H_3)] (X = CH_3, **[*m*-1b]**; X = $C(O)OCH_3$, **[*m*-1c]**; X = C≡C-4-C_6H_4-$C(O)OCH_3$, **[*m*-1d]**; X = C≡C-4-C_6H_4-NO_2, **[*m*-1e]**) were prepared by reaction of the iron chloride Cp*(dppe)FeCl (**4**) and the proligands **3b-e** obtained by a cross coupling reaction between the suitable aryl dibromides and trimethylsylilacethylene. After purification the complexes **[*m*-1b-e]** were isolated in yields ranging from 14 to 37 % and characterized by elemental analysis, high-resolution, ESI-mass spectra, multinuclear NMR, cyclic voltammetry, and IR spectroscopy. The complexes **[*m*-1b]**, **[*m*-1d]**, and **[*m*-1e]** were also characterized by XRD analyses on single crystals. The doubly oxidized complexes **[*m*-1b-e](PF$_6$)$_2$** were prepared (in ca. 64-87 % yields) by treatment of a CH_2Cl_2 solution of the corresponding neutral complexes **[*m*-1b-e]** with two equiv of [(C_5H_5)$_2$Fe](PF$_6$). The mixed-valence complexes (MV) **[*m*-1b-e](PF$_6$)** were obtained by comproportionation between one equiv of **[*m*-1b-e]** and one equiv of **[*m*-1b-e](PF$_6$)$_2$**. CV, IR and NIR data led to the conclusion that the MV **[*m*-1b-e](PF$_6$)** complexes are weakly coupled Class II MV derivatives and the distribution of the charge between the alkynyl iron centers and the phenyl ring might be tuned by the X-substituents in a limited extend.

Introduction

Molecules containing two redox active centers interacting through π-conjugated carbon rich framework constitute attractive potential components for use in future molecular electronics applications.[1-14]

Upon the years, three dinuclear organometallic molecules composed of two Cp*Fe(dppe) units bound about a central benzene ring with an ethynyl linker have been prepared.[15-17] These molecules (***p*-1**, ***o*-1**, ***m*-1**, Scheme 1) have the same molecular formula, but differ from each other in the geometry in which the metal centers are linked through the central phenyl ring.[18, 19] Sequential one-electron oxidation of these complexes results in Fe(II)-Fe(III) mixed-valence species and Fe(III)-Fe(III) diradicals.[15, 20-22] The topology of the molecules and in particular the *meta vs para* / *ortho* connection of the redox sites on the aromatic rings plays a major role on the electronic and magnetic coupling interactions.[18, 19, 23, 24]

In the case of the Fe(III-Fe(III) complexes antiferromagnetic exchange interactions take place between the spin carriers for the *ortho* and *para* topologies, while a strong ferromagnetic coupling is observed for the dicationic complex with the *meta* topology.[19, 23] In the case of the mixed-valence (MV) species Fe(II)-Fe(III), the electronic coupling between the two metal end-groups occurs directly via a through-bond mechanism.[25] However, the electronic coupling between the metal centers depends heavily on the topology of the molecules and decreases according to the sequence *para*, *ortho*, and *meta*.[17] In the three cases, the MV compounds are seen as localized MV species at the fast IR time scale, and consequently they belong to the Class-II systems according to Robin-Day classification.[22, 26, 27] At the slower Mössbauer time scale, the three complexes do not behave similarly. the *para* cationic complex is found to be symmetric with two equivalent formal Fe(2.5) metal centers, while the *ortho* and *meta* connected MV derivatives are characterized by discrete Fe(II) and Fe(III) centers.[15, 17, 21] Interestingly, at the single-molecule scale, the electron localization has only been observed for the MV species with the *meta* geometry by scanning tunneling microscopy (STM).[25]

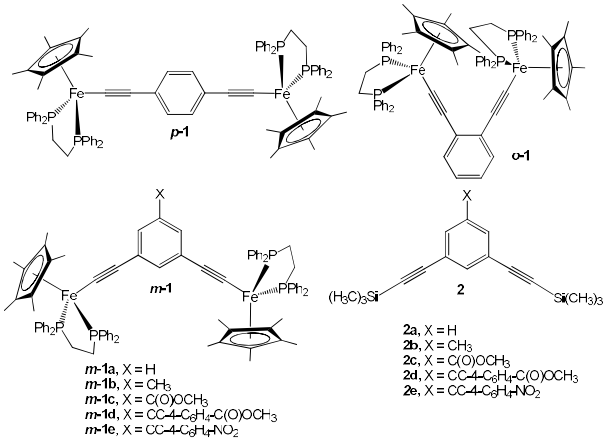

Scheme 1. General formulas of the key compounds.

Mixed-valence molecules with two discrete states constitute potential candidates for the elaboration of new devices for molecular electronics.[28, 29] As it was found that molecule **[*m*-1a]** presents some interesting properties at the single molecule level,[25] we have been interested to introduce some substituents in the 5-position of the central phenyl ring to evaluate its possible role on the electronic coupling. If the substituents can play a significant role, they could be helpful for tuning the metal-

[a] J. Lepont, Dr. T. Roisnel, Dr. J.-R. Hamon, Dr. Lapinte
Univ Rennes,
CNRS, ISCR-UMR 6226
35000 Rennes, France
E-mail: jean-rene.hamon@univ-rennes1.fr
claude.lapinte@ univ-rennes1.fr
https://iscr.univ-rennes1.fr/pmc/
https://twitter.com/chimie_iscr

Supporting information and ORCIDs from the authors for this article are available on the WWW under https://doi.org/

metal interaction through the bonding, otherwise they may open opportunities for introducing coordinating groups for the elaboration of supramolecular devices.

This paper is devoted to the synthesis of four binuclear organometallic molecules with a structure similar to **[*m*-1a]** and bearing a substituent X at the 5-position of the central aromatic ring, (X= CH_3, **[*m*-1b]**; X = $C(O)OCH_3$, **[*m*-1c]**; X = C≡C-4-C_6H_4-$C(O)OCH_3$, **[*m*-1d]**; X = C≡C-4-C_6H_4-NO_2, **[*m*-1e]**) and their full characterization including an X-ray diffraction study on single crystal for three of them. We also report the preparation of the doubly oxidized complexes **[*m*-1b-e](PF$_6$)$_2$** and their IR and NIR spectroscopic properties. The corresponding MV complexes **[*m*-1b-e](PF$_6$)** prepared by comproportionation have also been isolated and their electronic coupling determined from the analysis of the NIR spectra are discussed.

Results and Discussion

1. Synthesis of the Complexes [1,3-{Cp*(dppe)Fe-C≡C-}$_2$-5-(X)-(C_6H_3)] (X = CH_3, [*m*-1b]; X = $C(O)OCH_3$, [*m*-1c]; X = C≡C-4-C_6H_4-$C(O)OCH_3$, [*m*-1d]; X = C≡C-4-C_6H_4-NO_2, [*m*-1e])

The new complexes **[*m*-1b-e]** were obtained from the reaction of the iron chloride Cp*(dppe)FeCl (**4**) and the proligands **3b-e** following a procedure similar to that previously established for the preparation of the unsubstituted complex **[*m*-1a]**.[16] The proligands have been synthesized by a Pd/Cu-catalyzed cross coupling reaction using the commercially available or home made known aryl dibromides **2b-e** (Schemes 2 and 3).[30, 31]

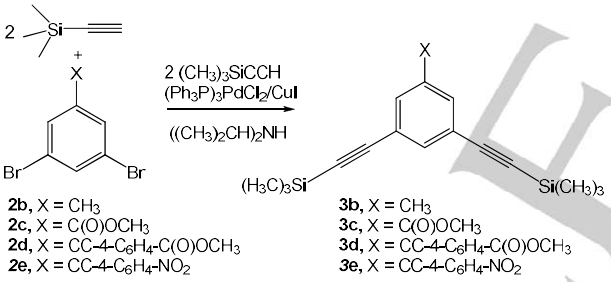

Scheme 2. Preparation of the proligands **3b-e**.

The crude samples of the new complexes were purified by extraction with CH_2Cl_2, precipitation and washing with pentane and crystallization by slow diffusion of pentane into saturated CH_2Cl_2 solutions of **[*m*-1b-e]**. This straightforward procedure provided analytically pure complexes with acceptable yields. The new complexes **[*m*-1b-e]** were characterized by mass spectrometry, multinuclear NMR (see Experimental Section), cyclic voltammetry, and IR spectroscopies (see Sections 3 and 4). Their bulk purity was determined through elemental analysis.

2. X-ray Crystal Structure of [1,3-{Cp*(dppe)Fe-C≡C-}$_2$-5-(X)-(C_6H_3)] (X = CH_3, [*m*-1b]; X = C≡C-4-C_6H_4-$C(O)OCH_3$, [*m*-1d]; X = C≡C-4-C_6H_4-NO_2, [*m*-1e])

Suitable crystals for X-ray analyses were obtained by slow diffusion of pentane into CH_2Cl_2 solutions for **[*m*-1b]**, **[*m*-1d]**, and **[*m*-1e]**. ORTEP views of these compounds are illustrated in Figure 1, while key structural parameters and X-ray data conditions are collected in Table S1 in the Supporting Information. Selected bond distances and bond angles for the Cp*(dppe)Fe-C≡C fragments and the organic bridges are given in Table S2 and Table S3, respectively. The asymmetric units contain 8, 4, and 4 molecules of **[*m*-1b]**, **[*m*-1d]**, and **[*m*-1e]**, respectively. In the case of **[*m*-1b]** two molecules (**[*m*-1bA]** and **[*m*-1bB]**) crystallographically nonequivalent are present in the unit cell. The asymmetric unit of **[*m*-1e]** also contains two molecules of CH_2Cl_2 which were refined, while disordered solvent molecules in crystals of **[*m*-1b]** and **[*m*-1d]** were squeezed (see Experimental Section).

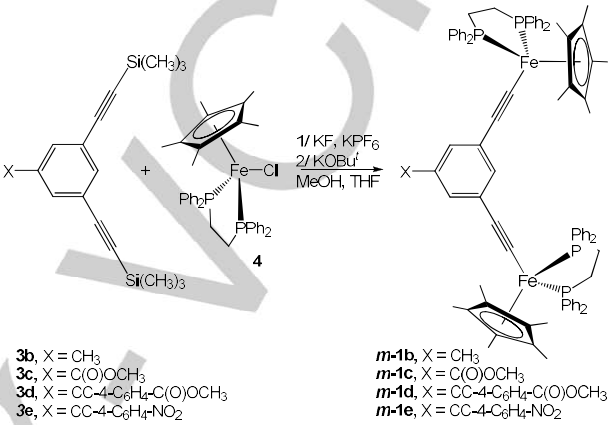

Scheme 3. Preparation of the complexes **[*m*-1b-e]**.

As expected, bond lengths in the Cp*(dppe)Fe fragments are typical, while angles confirm the pseudo-octahedral geometry of the metal atoms.[18, 19, 32] For the three complexes, the phenyl ring which connect the two iron alkynyl fragment is planar and this plan also contains the alkynyl carbon atoms in β-position with respect to the metal atoms, while the iron-alkynyl axes deviated above and below this plan. In compound **[*m*-1d]**, the two phenyl rings of the C_6-C≡C-C_6 fragment and the methyl ester are almost coplanar and can be modeled over two positions with equal occupancies by symmetry operations -x, -y, -z. The 11 atoms of the ethynyl paranitrobenzene fragment of the compound **[*m*-1e]** are almost coplanar and the dihedral angle between this plan and the plan of the phenyl ring connecting the iron alkynyl groups is close to 28 °.

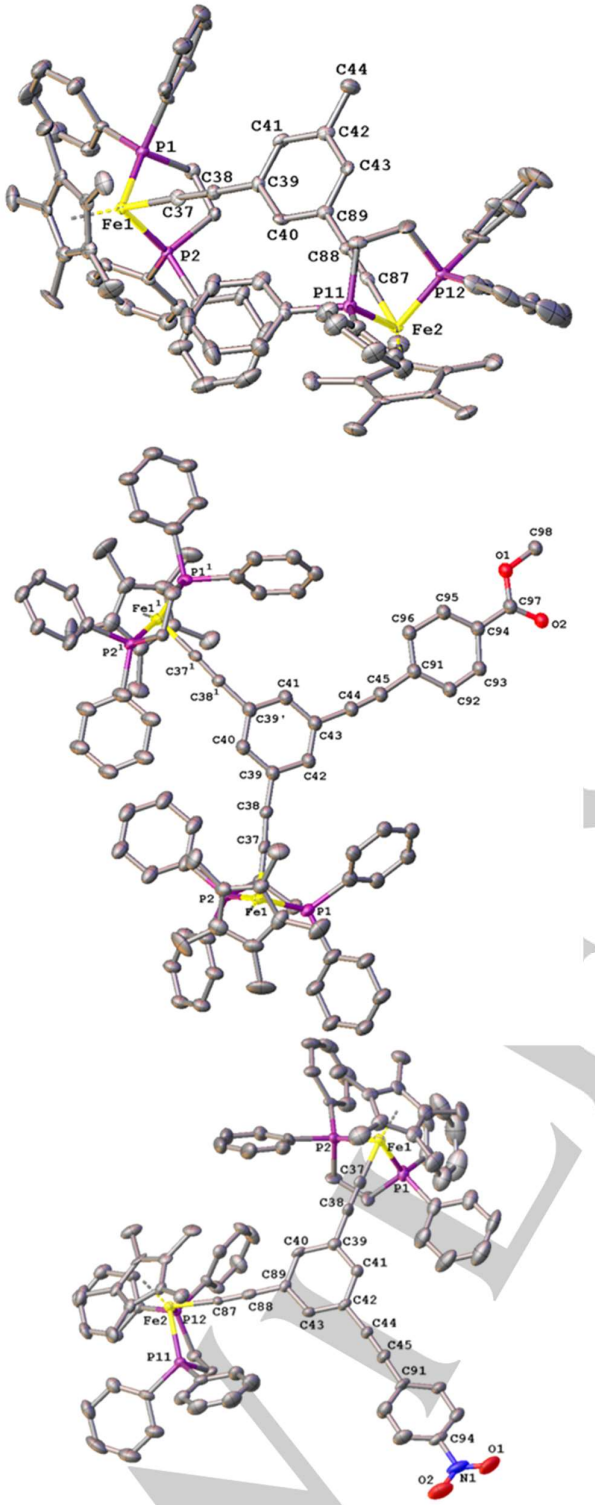

Figure 1. Molecular structures, from top to bottom: **[*m*-1b]** (molecule **A**, thermal ellipsoids at the 60% probability level), **[*m*-1d]** (thermal ellipsoids at the 40% probability level, symmetry equivalent and disordered atom are marked in superindex A^1 and A′, respectively, **[*m*-1e]**•$2CH_2Cl_2$, (thermal ellipsoids at the 60% probability level). Hydrogen atoms and crystallization solvent molecules have been omitted for clarity.

3. Cyclic Voltammetry Analysis and Preparation of the Dioxidized complexes [1,3-{Cp*(dppe)Fe-C≡C-}$_2$-5-(X)-(C_6H_3)](PF_6)$_2$ (X = CH_3, [*m*-1b](PF_6)$_2$; X = C(O)OCH_3, [*m*-1c](PF_6)$_2$; X = C≡C-4-C_6H_4-C(O)OCH_3, [*m*-1d](PF_6)$_2$; X = C≡C-4-C_6H_4-NO_2, [*m*-1e](PF_6)$_2$)

The initial scans in the cyclic voltammetry of the binuclear complexes **[*m*-1b-e]** were run from -1.0 to 1.0 V (vs SCE). The cyclic voltammograms display two partially separated and fully reversible waves as shown in Figure 2 for the bis(iron) compound **[*m*-1d]** taken as a representative example of the series. The electrochemical data are collected in Table 1. The current peak ratio of unity (i_p^a/i_p^c = 1) for the two waves indicates that the two successive one-electron oxidations yield the Fe(II)-Fe(III) and the Fe(III)-Fe(III) species which are thermally stable at the platinum electrode. As shown in Table 1, the anodic and cathodic peak separation is close to 0.060 V for the two waves with a scan rate of 0.100 V s^{-1} indicating that the electron transfer is fast and the structural reorganization around the redox centers is not important.[33]

Table 1. Electrochemical Data for Compounds **[*m*-1a-e]** and Molar Fraction of the Species (x^{n+}) in Solution of the Mixed-Valence complexes at 20 °C[a]

Cpd.	$E^0_1(\Delta E_p)$	$E^0_2(\Delta E_p)$	ΔE^0	K_c	x	x^+	x^{2+}
[*m*-1a][b]	-0.23(0.08)	-0.10(0.08)	0.13	130	0.07	0.85	0.07
[*m*-1b]	-0.25(0.06)	-0.10(0.06)	0.15	275	0.05	0.89	0.05
[*m*-1c]	-0.18(0.06)	-0.05(0.06)	0.13	130	0.07	0.85	0.07
[*m*-1d]	-0.17(0.06)	-0.05(0.06)	0.12	110	0.08	0.84	0.08
[*m*-1e]	-0.16(0.06)	-0.04(0.06)	0.12	110	0.08	0.84	0.08

[a] $\Delta E^0 = E^0_2 - E^0_1$ in V vs SCE obtained from CV on Pt electrode at 20 °C in CH_2Cl_2 with 0.1 M $NBu^n_4PF_6$, sweep rate 0.100 V s^{-1}; the ferrocene-ferricinium couple (0.460 V vs SCE)[34] was used as an internal reference for the potential measurements. [b]From [15].

The more negative redox potential found for the first oxidation (E^0_1) of the compound **[*m*-1b]** than for the parent compound **[*m*-1a]** shows that the electron releasing property of the methyl substituent is sensed by the iron centers. In contrast, the E^0_1 values continuously decrease from **[*m*-1a]** to **[*m*-1c]**, **[*m*-1d]**, and **[*m*-1e]** in accord with the electron withdrawing character of the X substituents. Similarly, the redox potential of the second metal center is also influenced by the electronic properties of X. However, the slightly smaller effect of the substituents on the second redox potential contributes to decrease the potential difference (ΔE^0), and as a consequence, the constants K_c (derived from eq 1) for the comproportionation equilibria (eq 2) which decrease as the electron withdrawing character of the X substituents increases.

$$\Delta E^0 = RT/F \ln K_c \quad (1)$$

$$Fe^{II}\text{-L-}Fe^{II} + [Fe^{III}\text{-L-}Fe^{II}]^{2+} \rightleftharpoons 2\ [Fe^{II}\text{-L-}Fe^{III}]^{+} \quad (2)$$

For MV complexes with identical redox centers, the Kc value is related to the thermodynamic stability of the MV complex with respect to its homovalent relatives. This parameter comprises

several terms, such as the through-bridge and through-space electronic interactions, solvation, ion pairing, steric interaction, structural distortion upon electron transfer, magnetic coupling in diradicals.[4, 35-37] The K_c values determined for this series of complexes range between 110 and 275. Considering the *meta*-phenylene topology of this family of compounds, and the data available in the literature for other derivatives with the same topology,[38, 39] the K_c constants collected in Table 1 are rather large. As previously proposed, the relatively strong electronic interaction which takes place between the iron alkynyl units is probably favored by a continuous overlap between the *d* orbitals of the metal centers and the orbitals of the polyethynylbenzene connector. It is interesting to note that the most relevant system $Cl(dppe)_2FeC{\equiv}C\text{-}1,3\text{-}C_6H_4\text{-}C{\equiv}CFe(dppe)_2Cl$ investigated by Long *et al.* is characterized by similar data.[39]

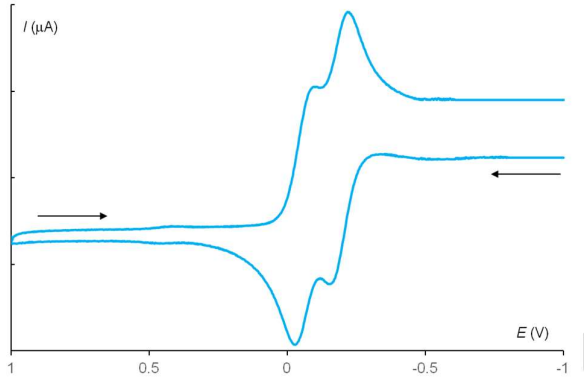

Figure 2. Cyclic voltammogram of **[*m*-1d]** (10^{-3} M in CH_2Cl_2 at 293 K, 0.1 M $[Bu^n_4N](PF_6)$, scan rate 0.100 V s^{-1}).

The molar fraction x^{n+} of the three species $[Fe\text{-}L\text{-}Fe]^{n+}$ (*n* = 0-2) of the equilibrium represented in eq. 2 were computed (Table 1, see Experimental Section). Clearly, for CH_2Cl_2 solution of the MV complexes **[*m*-1a-e](PF$_6$)**, the MV form predominate and the associated homovalent species range between 5 and 8 % each depending on the 5-X substituent.

Guided by the redox potentials, the preparation of the doubly oxidized complexes **[*m*-1b-e](PF$_6$)$_2$** were achieved by treatment of a CH_2Cl_2 solution of the corresponding neutral complexes with two equiv of $[(C_5H_5)_2Fe](PF_6)$. The reaction is rapid and immediately the initial orange color of the mixture turned to deep green. More slowly, the development of the final deep blue color can be observed. After completion, dark blue limpid solutions were obtained and addition of pentane gave dark blue microcrystals of the Fe(III)-Fe(III) complexes **[*m*-1b-e](PF$_6$)$_2$** isolated in ca. 80 % yields. The analytically pure samples of **[*m*-1b-e](PF$_6$)$_2$** were characterized by CV, IR and NIR spectroscopy, and mass spectrometry. Despite numerous efforts, it was not possible to grow single crystals for X-ray analysis.

Table 2. IR Bond Stretching for **[*m*-1a-d](PF$_6$)$_n$** (*n* = 0 - 2)

Cpd.	Fe-C≡C	Ar-C≡C-Ar	C=O	C-O	N-O
[*m*-1a]	2049[a] (s)				
[*m*-1a](PF$_6$)	2044[a] 1998[a]				
[*m*-1a](PF$_6$)$_2$	2006[a] (br)				
[*m*-1b]	2097 (w) 2055 (vs)				
[*m*-1b](PF$_6$)	2040 (s) 1944 (s)				
[*m*-1b](PF$_6$)$_2$	2004 (w) 1944 (s)				
[*m*-1c]	2050 (vs) 1980 (sh)		1713 (vs)	1216 (vs)	
[*m*-1c](PF$_6$)	2045 (vs) 1955 (w)		1716 (vs)	1223 (vs)	
[*m*-1c](PF$_6$)$_2$	2016 (vw) 1954 (w)		1716 (s)	1232 (s)	
[*m*-1d]	2046 (vs)	2210 (s)	1723 (vs)	1270 (vs)	
[*m*-1d](PF$_6$)	2039 (vs) 1950 (s)	2210 (w)	1718 (vs)	1274 (vs)	
[*m*-1d](PF$_6$)$_2$	2017 (vw) 1949 (w)	2214 (vw)	1718 (vs)	1274 (vs)	
[*m*-1e]	2048 (vs)	2209 (s)			1560 (s) 1345 (s)
[*m*-1e](PF$_6$)	2040 (s) 1951 (w)	2210 (w)			1561 (s) 1344 (s)
[*m*-1e](PF$_6$)$_2$	2013 (vw) 1946 (w)	2217 (vw)			1569 (s) 1343 (s)

[a]From [20]. br, broad; s, strong; vs, very strong; w, weak; vw, very weak.

The MV complexes **[*m*-1b-e](PF$_6$)** can be prepared either by reaction of the parent Fe(II)-Fe(II) complexes with 1 equiv of ferrocenium hexafluorophosphate or from the comproportionation reaction between the neutral and dicationic species as depicted in eq. 2. The second route was preferred, and 1 equiv of the Fe(II)-Fe(II) orange complexes **[*m*-1b-e]** and 1 equiv of the corresponding Fe(III)-Fe(III) dark blue derivatives **[*m*-1b-e](PF$_6$)$_2$** were introduced as powders in a Schlenk tube. In the solid state, the reaction does not take place between the orange and dark blue powders, but as soon as CH_2Cl_2 was introduced, the characteristic dark green color of the MV complexes can be observed. The mixtures were stirred at 20 °C until the formation of limpid solutions and the solvent was removed under reduced pressure to dryness. The resulting dark green powders of the MV complexes **[*m*-1b-e](PF$_6$)** obtained from analytically pure homovalent parents were supposed to be pure and used for IR and NIR measurements (see Sections 4 and 5) without further treatment. Attempts to grow crystals by slow diffusion of pentane into CH_2Cl_2 solution of the MV complexes led to the precipitation of Fe(III)-Fe(III) complexes and the formation of orange liquors containing the Fe(II)-Fe(II) relatives leading to the quantitative recovery of the starting materials in their pure form.

4. Infrared Spectroscopy for [*m*-1a-e](PF$_6$)$_n$ (*n* = 0 - 2)

The IR spectra were recorded for the neutral, mono-oxidized and doubly oxidized binuclear complexes **[*m*-1b-e](PF$_6$)$_n$** (*n* = 0 -

2) and compared with the data available in the literature for **[*m*-1a](PF$_6$)$_n$** (Table 2). The IR spectra of the Fe(II)-Fe(II) neutral complexes **[*m*-1a-e]** show an intense bond stretching characteristic of the Fe^{II}-C≡C triple bond at a frequency which slightly varies with the electronic properties of the X substituents between 2045 and 2052 cm^{-1}. In the cases of **[*m*-1b]** and **[*m*-1c]**, a second much less intense absorption is observed. These bands could be assigned to the asymmetric and symmetric modes of vibration of the two Fe-C≡C fragments, respectively.

In the case of the doubly oxidized Fe(III)-Fe(III) related derivatives **[*m*-1b-e](PF$_6$)$_2$**, the IR spectra display two less intense absorptions which can be assigned to the Fe^{III}-C≡C vibrators. The energy of the more intense band ranges between 1944 and 1954 cm^{-1} and can be tentatively assigned to the antisymmetric mode of vibration, while the less intense band is seen at higher frequencies (2004 - 2017 cm^{-1}) and should correspond to the symmetric mode.

The electronic properties of the X subsituents have a small, but measurable effect on the energy of the Fe-C≡C stretch (ca. 5 cm^{-1}), and reciprocally, the oxidation of the metal centers is sensed by the whole molecule. In particular, upon the double oxidation of the complexes, the frequency of vibration of the C≡C triple bond which link the two aromatic rings in **[*m*-1d-e](PF$_6$)$_n$** is shifted toward higher energy by 4 to 8 cm^{-1}. Similarly, the C=O, C-O, and N-O bands are also slightly shifted toward higher energies (Table 2). These observations suggest that the X substituents play a sizeable role on the electronic structure of these complexes, and they can tune the charge distribution between the Fe-C≡C units and the bridge which connect them.

As previously reported for **[*m*-1a](PF$_6$)**, the IR spectra of the MV complexes **[*m*-1b-e](PF$_6$)** show two distinct $\nu_{C\equiv C}$ stretching bands located around 2040±5 and 1950±5 cm^{-1}, which can be safely ascribed to the Fe^{II}-C≡C and Fe^{III}-C≡C vibrators, respectively. They constitute the spectroscopic signature for trapped MV complexes. The characteristic stretching bands of the C≡C triple bond, C=O and C-O double and single bonds, and N-O bonds of the X substituents are located in the IR spectra of the MV derivatives at intermediate frequencies between those found for the corresponding homovalent counterparts. As a result, one can anticipate that the substituents at the 5-position of the phenyl ring connecting the charge carriers might modulate the rate of the intramolecular electron transfer between the redox active sites. The analysis of the NIR absorptions characteristics of the MV complexes should confirm this assumption.

5. Near Infrared Spectroscopy for [*m*-1a-e](PF$_6$)$_n$ (*n* = 0 - 2)

As invariably noted for the Fe(II) complexes, the NIR spectra of the neutral complexes **[*m*-1a-e]** do not contain any absorption between 3700 and 12000 cm^{-1}.[18, 19] As expected, the NIR spectra of the dioxidized complexes **[*m*-1a-e](PF$_6$)$_2$** show a weak band (ε < 150 M^{-1} cm^{-1}) with a maximum around 5300 ± 100 cm^{-1}, safely assigned to the forbidden ligand field (LF) transition from the (SOMO-2) to the SOMO).[40]

The experimental spectra of the mono-oxidized complexes **[*m*-1b-e](PF$_6$)** collected from isolated samples of the MV complexes (see Experimental Section) display absorptions of weak intensities with complex shapes. As previously described for **[*m*-1a](PF$_6$)** and other related compounds,[21, 41-44] the deconvolution of the spectra was achieved using Gaussian functions. The spectra are mainly the combination of three overlapping components and their energetic parameters (ν_{max} = frequency at the maximum of absorption, $\Delta\nu_{1/2}$ = broadness at half height) are collected in Table 3. The low energy band found between 5330 (**[*m*-1b](PF$_6$)**) and 5380 cm^{-1} (**[*m*-1c-e](PF$_6$)**) with an extinction coefficient around 100 M^{-1} cm^{-1} is almost independent of the substituent bound to the 5-position of the phenyl ring. This band, characteristic of the Fe(III) cation of the MV complexes, is assigned to a LF transition. The two other components, which do not exist in the spectra of the corresponding homovalent species, result from the weak coupling taking place between the two iron alkynyl entities through the central phenyl ring.

Table 3. NIR data for **[*m*-1a-e](PF$_6$)** in CH_2Cl_2.

Cpd	transition	ν_{max} (cm^{-1})	$\Delta\nu_{1/2}$
[*m*-1a](PF$_6$)[a]	LF	5350	1050
	Fe^{II}C≡C → Fe^{III}-C≡C	5400	3700
	Fe^{II}C≡C → Fe^{III}-C≡C	10000	3700
[*m*-1b](PF$_6$)	LF	5330	1350
	Fe^{II}C≡C → Fe^{III}-C≡C	7450	1950
	Fe^{II}C≡C → Fe^{III}-C≡C	11280	1950
[*m*-1c](PF$_6$)	LF	5380	1350
	Fe^{II}C≡C → Fe^{III}-C≡C	5450	2220
	Fe^{II}C≡C → Fe^{III}-C≡C	13020	2220
[*m*-1d](PF$_6$)	LF	5380	1250
	Fe^{II}C≡C → Fe^{III}-C≡C	9020	2500
	Fe^{II}C≡C → Fe^{III}-C≡C	13020	2500
[*m*-1e](PF$_6$)	LF	5380	1250
	Fe^{II}C≡C → Fe^{III}-C≡C	8600	2600
	Fe^{II}C≡C → Fe^{III}-C≡C	12800	2600

[a]From [21].

Following assignments proposed for **[*m*-1a](PF$_6$)** with the support of DFT calculations, these bands can be assigned to Fe^{II}-C≡C → Fe^{III}-C≡C transitions. The MV complexes, all weakly coupled, belong to the Robin-Day Class II MV species,[45] however the presence of X substituents on the phenyl ring can shift the bands by almost 3000 cm^{-1}. This observation shows that the X-substituents finely tune the distribution of the charge between the iron alkynyl fragments and the phenyl ring.

Conclusions

The new complexes [1,3-{Cp*(dppe)Fe-C≡C-}$_2$-5-(X)-(C$_6$H$_3$)](PF$_6$)$_n$ (X = CH$_3$, **[*m*-1b](PF$_6$)$_n$**; X = C(O)OCH$_3$, **[*m*-1c](PF$_6$)$_n$**; X = C≡C-4-C$_6$H$_4$-C(O)OCH$_3$, **[*m*-1d](PF$_6$)$_n$**; X = C≡C-4-C$_6$H$_4$-NO$_2$, **[*m*-1e](PF$_6$)$_n$**) were prepared, isolated, and characterized for *n* = 0-2. The analyses by CV, IR and NIR spectroscopies establish that the electronic properties are weakly sensed by the metal centers through five bonds and even eleven bonds in the cases of the complexes **[*m*-1d](PF$_6$)$_n$** and **[*m*-1e](PF$_6$)$_n$**. Reciprocally, the spectroscopic data also show that the X substituents sensed the oxidation of the metal centers. However, the transmission of the electronic properties of the substituents in the 5-position of the phenyl ring to the metal centers is too weak to allow the tuning of the metal-metal interaction. In contrast, advantage can be taken from this result to introduce coordinating groups in that position and elaborate supra molecular structures. This will be the subject of future reports from our group.

Experimental Section

Experimental Details: Manipulations of air-sensitive compounds were performed under an argon atmosphere using standard Schlenk techniques. Tetrahydrofuran (THF), toluene and pentane were dried and deoxygenated by distillation from sodium/benzophenone ketyl. Dichloromethane was distilled under argon from P_2O_5 and then from Na_2CO_3. Methanol was distilled over dried magnesium turnings. Infrared spectra were obtained as KBr pellets with a Bruker Alpha FTIR infrared spectrophotometer (4000-400 cm^{-1}). Near-IR and UV-visible spectra were recorded as CH_2Cl_2 solutions, using a 1 cm long quartz cell on a Cary 5000 spectrophotometer. ^1H, ^{13}C, and ^{31}P NMR spectra were acquired on a Bruker AVIII 300 multinuclear NMR spectrometer at ambient temperature. Chemical shifts are reported in parts per million (δ) relative to tetramethylsilane (TMS), using the residual solvent resonances as internal references for ^1H and ^{13}C and external H_3PO_4 (0.0 ppm) for ^{31}P NMR spectra. Carbon atoms are numbered as shown on Scheme 4 for assignment of the NMR spectra.

Scheme 4. Atom numbering for assignment of the NMR spectra.

Coupling constants (*J*) are reported in Hertz (Hz). High resolution electro-spray ionization mass spectra (HRMS ESI) were acquired on Bruker MAXI 4G and Thermo Fisher Scientific Q-Exactive spectrometers, operating in the positive mode. Cyclic voltammograms were recorded in dry CH_2Cl_2 solutions containing 0.1 M $[Bu^n_4N](PF_6)$ as supporting electrolyte, purged with argon and maintained under argon atmosphere, using a EG&G-PAR model 362 potentiostat/galvanostat. The working electrode was a Pt disk, the counter electrode a Pt wire and the reference electrode a saturated calomel electrode. The ferrocene/ferrocenium redox couple ($E_{1/2}$ = 0.46 V) was used as an internal calibrant for the potential measurements.[34] Elemental analyses were conducted on a Thermo-Finnigan Flash EA 1112 CHNS/O analyzer.

Chemicals: The organic compounds **2b**, **2c**, 1-bromo-4-ethylbenzoate, 1-bromo-4-nitrobenzene, trimethylsilylacetylene, bis(triphénylphosphine)palladium dichloride, cuprous iodide, diisopropylamine, potassium tert-butoxide, potassium fluoride and potassium hexafluorophosphate were purchased from Acros Organics, Alfa Cesar or Aldrich Chemicals, and used as received without further purification. 1-iodo-3,5-dibromobenzene,[46] 1-ethynyl-4-ethylbenzoate,[47] 1-ethynyl-4-nitrobenzene,[48] and Cp*(dppe)FeCl (**4**).[49] were prepared following reported procedures.

Calculation of the Molar Fraction x^{n+}. Let us consider the equilibrium shown in eq 2. The comproportionation constants are $Kc1 = [x^+]^2/[x][x^{2+}]$. The conservation of masses and charges provides two other equations: $[x] + [x^+] + [x^{2+}] = 1$ and $[x^+] + 2[x^{2+}] = n$, n being the number of metal centers oxidized. The system of equations was solved by successive iterations using a Excel worksheet and a lap top.

Ethyl 4-((3,5-dibromophenyl)ethynyl)benzoate (2d): A Schlenk tube equipped with a reflux condenser was charged with ethyl 4-ethynylbenzoate (1.044 g, 6.0 mmol), 1, 1-iodo-3,5-dibromobenzene (2.159 g, 6.0 mmol), bis(triphénylphosphine)palladium dichloride (0.421 g, 0.60 mmol), CuI (0.057 g, 0.30 mmol), 40 mL of THF and 20 mL of diisopropylamine. The reaction mixture was stirred at 60 °C for 16h. Upon cooling to room temp., the solvents were evaporated and the residue purified by column chromatography on silica gel eluting with a pentane/CH_2Cl_2 mixture (3:2). The solvents were removed in vaccuo to give a brown oil (0.914 g, 2.25 mmol, 38% yield). ^1H NMR (300 MHz, $CDCl_3$): δ = 8.06 (d, $^3J_{H,H}$ = 8.4 Hz, 2H; Ph), 7.69-7.57 (m, 5H; Ph), 4.42 (q, $^3J_{H,H}$ = 7.1 Hz, 2H; CH_2), 1.43 ppm (t, $^3J_{H,H}$ =7.1 Hz, 3H; CH_3); IR (KBr): $\bar{\upsilon}$ = 2197, 1714, 1272 cm^{-1}; HRMS (ESI): m/z calcd for $C_{17}H_{13}Br_2O_2^+$: 406.92768 $[M]^+$; found: 406.9283.

1,3-dibromo-5-((4-nitrophenyl)ethynyl)benzene (2e): A Schlenk tube equipped with a reflux condenser was loaded with 1-iodo-3,5-dibromobenzene (0.733 g, 2.04 mmol), 4-nitrophenylacetylène (0.439 g, 2.99 mmol), bis(triphénylphosphine)palladium dichloride (0.141 g, 0.20 mmol), CuI (0.019 g, 0.10 mmol) and 20 mL of diisopropylamine. The reaction was stirred at 30 °C for 16h. At room temp., the solvent was removed under reduced pressure and the residue purified by column chromatography on silica gel, eluting with pentane. The solvent was evaporated and the solid residue dried under vacuum to give 0.404 g (1.07 mmol, 53.5 % yield) of a yellowish powder. ^1H NMR (300 MHz, $CDCl_3$): δ = 8.24 (m, 2H; Ph), 7.67 (m, 5H; Ph); IR (KBr): $\bar{\upsilon}$ = 2163, 1510, 1337 cm^{-1}; HRMS (ESI): m/z calcd for $C_{14}H_7BR_2NO_2^+$: 379.89218 $[M]^+$; found: 379.8910.

[1,3-{$(CH_3)_3Si$-C≡C-}$_2$-5-(CH_3)-(C_6H_3)] (**3b**) : A Schlenk tube equipped with a reflux condenser was charged with 1.250 g (5.0 mmol) of 1-methyl-3,5-dibromobenzene (**2b**), 175 mg (0.25 mmol) of bis(triphénylphosphine)palladium dichloride, 47.6 mg (0.25 mmol) of CuI), 40 mL of THF, 20 mL of diisopropylamine, and the reagents were mixed for 5 min. Then, 1.52 mL (11.0 mmol) of trimethylsylilacetylene was added and the reaction mixture was stirred at 90°C for 15 h. The volatiles were removed under reduced pressure, and the solid residue was purified by column chromatography on silica gel eluting with pentane. Upon evaporating the solvent under reduced presure, a colorless oil was obtained (1.065 g, 3.75 mmol, 75% yield). ^1H NMR (300 MHz, $CDCl_3$): δ = 7.40 (m, 1H; H_6), 7.23 (m, 2H; H_4), 2.28 (s, 3H; CH_3), 0.24 ppm (s, 18H; $Si(CH_3)_3$); ^{13}C NMR (75 MHz, $CDCl_3$): δ = 137.96 (C_5), 132.59(C_6), 132.52 (C_4), 123.19 (C_7), 104.34 (C_3), 94.38 (C_2), 20.91 (CH_3), -0.05 ppm ($Si(CH_3)_3$); IR (KBr): $\bar{\upsilon}$ = 2158 (s) (C≡C), 2123 (w) cm^{-1} (C≡C); HRMS (ESI): m/z calcd for $C_{17}H_{25}Si_2^+$: 285.14893 $[M+H]^+$; found: 285.1487.

[1,3-{$(CH_3)_3Si$-C≡C-}$_2$-5-$(C(O)OCH_3)$-(C_6H_3)] (**3c**): A Schlenk tube equipped with a reflux condenser was charged with 1057 mg (3.40 mmol) of 1,3-dibromo-5-methylbenzoate (**2c**), 119 mg (0.17 mmol) of bis(triphénylphosphine)palladium dichloride, 32 mg (0.17 mmol) of CuI, 30 mL of THF, 15 mL of diisopropylamine. The reagents were mixed for 5 min. Then, 0.99 mL (7.14 mmol) of trimethylsylilacetylene was added by syringe and the mixture was stirred at 90°C for 15 h. At room temp., the volatiles were removed under reduced pressure, and the solid residue was purified by column chromatography on silica gel, eluting with pentane/CH_2Cl_2 (3:2). The solvents were removed under reduced presure to give a colourless oil (951 mg, 2.90mmol, 85% yield). ^1H NMR (300 MHz, $CDCl_3$): δ = 8.04 (d, $^4J_{H,H}$ = 1.6 Hz, 2H; H_2), 7.72 (t, $^4J_{H,H}$ = 1.6 Hz, ^1H; H_3), 3.91 (s, 3H; OCH_3), 0.24 ppm (s, 18H; $Si(CH_3)_3$); ^{13}C NMR (75 MHz, $CDCl_3$): δ = 165.63 ($C(O)$), 138.99 (C_5), 132.62 (C_6), 130.54 (C_4), 123.89 (C_7), 102.93 (C_3), 96.13 (C_2), 52.3 (CH_3), -0.20 ppm ($Si(CH_3)_3$); IR (KBr): $\bar{\upsilon}$ = 2159 (s) (C≡C), 2118 (w) (C≡C), 1729 (s) cm^{-1} (C=O); HRMS (ESI): m/z calcd for $C_{18}H_{25}O_2Si_2^+$: 329.13876 $[M+H]^+$; found: 329.1391.

[1,3-{$(CH_3)_3Si$-C≡C-}$_2$-5-(1,4-C≡C-4-C_6H_4-$C(O)OCH_2CH_3$)-(C_6H_3)] (**3d**): A Schlenk tube equipped with a reflux condenser was charged with ethyl 4-((3,5-dibromophenyl)ethynyl)benzoate (**2d**), 0.914 g (2.25 mmol), bis(triphénylphosphine)palladium dichloride (0.158 g, 0.225 mmol), CuI (21 mg, 0.1125 mmol), 40 mL of THF, 20 mL of diisopropylamine. The reagents were mixed for 5 min. Trimethylsylilacetylene (0.68 mL, 4.95 mmol) was added by syringe and the reaction mixture was stirred at 90°C for 16 h. Then, the volatiles were removed under reduced pressure, and

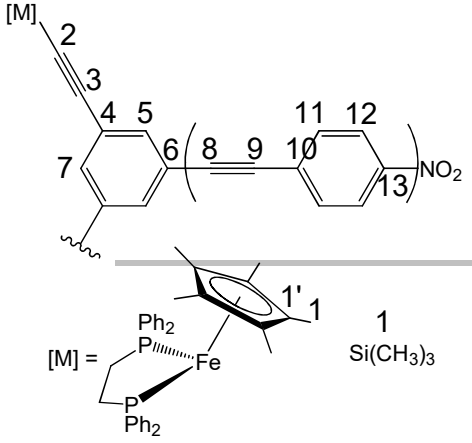

the residue was purified by column chromatography on silica gel eluting with pentane/CH_2Cl_2 (3:2). Evaporation of the solvents gave a brown oil (800 mg, 1.81 mmol, 80% yield). ^{1}H NMR (300 MHz, $CDCl_3$): δ = 8.06 (d, $^3J_{H,H}$ = 8.42 Hz, 2H; H_9), 7.66 (M, 3H; H_1, H_3), 7.59 (d, $^3J_{H,H}$ = 8.42 Hz, 2H; H_8), 4.41 (q, $^3J_{H,H}$ = 7.05 Hz, 2H; *CH*$_2$), 1.43 (t, $^3J_{H,H}$ = 7.2 Hz, 3H; *CH*$_3$), 0.27 ppm (s, 18H; $Si(CH_3)_3$); ^{13}C NMR (75 MHz, $CDCl_3$): δ = 165.85, *C(O)*), 135.16 (*C*$_{13}$), 134.59 (C_{12}), 131.50 (*C*$_{11}$), 130.18 (*C*$_{10}$), 129.51 (C_5), 127.28 (*C*$_6$), 123.93 (*C*$_4$), 123.28 (*C*$_7$), 103.07 (*C*$_9$), 95.89 (*C*$_8$), 90.42 (*C*$_3$), 89.66 (*C*$_2$), 61.11 (CH_2), 14.31 (CH_2-$\underline{C}H_3$), 0.18 ppm (*C*$_1$); IR (KBr): $\bar{\upsilon}$ = 2217 (w) (C≡C), 2157 (s) (C≡C), 2143 (w) (C≡C), 1724 (s) cm^{-1} (C=O); HRMS (ESI): m/z calcd for $C_{27}H_{30}O_2NaSi_2^+$: 465.16766 $[M+Na]^+$; found: 465.1677.

[1,3-{$(CH_3)_3$Si-C≡C-}$_2$-5-(1,4-C≡C-C_6H_4-NO_2)-(C_6H_3)] (**3e**): A Schlenk tube equipped with a reflux condenser was charged with 370 mg (0.98 mmol) of 1,3-dibromo-5-((4-nitrophenyl)ethynyl)benzene (**2e**), 72 mg (0.1 mmol) of bis(triphénylphosphine)palladium dichloride, 9.5 mg (0.05 mmol) of CuI, 20 mL of diisopropylamine. The reagents were mixed for 5 min. Then, 0.30 mL (2.5 mmol) of trimethylsylilacetylene was added by syringe and the reaction mixture was stirred at 90°C for 23h. The volatiles were removed under reduced pressure, and the residue was purified by column chromatography on silica gel, eluting with pentane. Evaporation of the solvent gave a yellowish powder (323 mg, 0.78 mmol, 80% yield). ^{1}H NMR (300 MHz, $CDCl_3$): δ = 8.24 (d, $^3J_{H,H}$= 8.82 Hz, 2H; *H*$_{12}$), 7.65 (d, $^3J_{H,H}$= 8.82 Hz, 2H; *H*$_{11}$), 7.60 (M, 3H; H_5, H_6), 0.27 ppm (s, 18H; $Si(CH_3)_3$); ^{13}C NMR (75 MHz, $CDCl_3$): δ = 147.25 (*C*$_{13}$), 135.69 (*C*$_{10}$), 134.67 (*C*$_{12}$), 132.36 (*C*$_{11}$), 129.67 (*C*$_6$), 124.07 (*C*$_5$), 123.70 (*C*$_4$), 122.63 (*C*$_7$), 102.84 (*C*$_9$), 96.23 (*C*$_8$), 92.78 (*C*$_3$), 88.68 (*C*$_2$), 0.20 ppm (*C*$_1$); IR (KBr): $\bar{\upsilon}$ = 2216 (w) (C≡C), 2159 (s) (C≡C), 2137 (w) (C≡C), 1519 (s) (N-O), 1343 (s) cm^{-1} (N-O); HRMS (ESI): m/z calcd for $C_{24}H_{25}NO_2NaSi_2^+$: 438.13161 $[M+Na]^+$; found: 438.1321.

[1,3-{Cp*(dppe)Fe-C≡C-}$_2$-5-(CH_3)-(C_6H_3)] (**[*m*-1b]**): A Schlenk tube equipped with a reflux condenser was charged with **3b** (0.568 g, 2 mmol), KF (0.274 g, 4.72 mmol), KPF_6 (0.869 g, 4.72 mmol), MeOH (40 mL) and THF (4 mL). The reagents were stirred for 5 min at 20 °C. Then, Cp*(dppe)FeCl (2.945 g, 4.72 mmol) was added and the mixture was stirred at 90 °C for 16 h. After cooling to room temp., the solution was treated with KOBu^t for 30 min. The solvents were removed under reduced pressure, and the solid residue was extracted with dichloromethane (3 x 30 mL). The extracts were evaporated to dryness and the solid residue was washed with pentane (2 x 20 mL) and dried under vacuum. Slow diffusion of pentane into a saturated solution of **[*m*-1b]** in dichloromethane afforded red-orange crystals (0.369 g, 0.28 mmol, 14 % yield). A single crystal of this crop was selected and used for X-ray diffraction analysis. ^{1}H NMR (300 MHz, CD_2Cl_2): δ = 7.97-7.31 (m, 40H; Ph/dppe), 6.39 (s, 1H; H_7), 6.13 (s, 2H; H_5), 2.70 (m, 4H; CH_2/dppe), 2.05 (m, 4H, CH_2/dppe), 2.03 (s, 3H; CH_3), 1.45 ppm (s, 30H; H_1); ^{13}C NMR (75 MHz, CD_2Cl_2): δ = 138.71 (t, $^2J_{C,P}$ = 36 Hz; C_2), 135.42 (s, C3), 134.26-127.01 (Ph), 87.47 (s, *C*$_{1'}$), 30.62 (m, CH_2/dppe), 21.03 (s, CH_3), 9.86 ppm (s, C_1); ^{31}P NMR (120 MHz, CD_2Cl_2): δ = 99.91 ppm (s, dppe); IR (KBr): $\bar{\upsilon}$ = 2097 (*w*) (C≡C), *2055* (*s*) (C≡C); HRMS (ESI): m/z calcd for $C_{83}H_{84}{}^{56}Fe_2P_4^+$: 1316.42169 $[M]^+$; found: 1316.4223; elemental analysis calcd (%) for $C_{83}H_{84}Fe_2P_4$•$2CH_2Cl_2$: C 68.66, H 5.96; found: C 68.46, H 5.76.

[1,3-{Cp*(dppe)Fe-C≡C-}$_2$-5-($C(O)OCH_3$)-(C_6H_3)] (**[*m*-1c]**): A Schlenk tube equipped with a reflux condenser was charged with **3c** (0.657 g, 2.0 mmol), KF (0.274 g, 4.72 mmol), KPF_6 (0.869 g, 4.72 mmol), MeOH (40 mL) and THF (4 mL), and the reagents were stirred for 5 min. Then Cp*(dppe)FeCl (2.945 g, 4.72 mmol) was added, the mixture was stirred at 90°C for 16 h. After cooling to 20 °C, the solution was treated with KOBu^t. The solvents were removed under reduced pressure, and the solid residue was extracted with dichloromethane (3 x 30 mL). The extracts were evaporated to dryness and the solid residue was washed with pentane (2 x 20 mL) and dried under vacuum. Slow diffusion of pentane into a saturated solution of ***[m*-1c]** in dichloromethane afforded a red-orange microcrystalline powder (0.76 g, 0.56 mmol, 28 % yield). ^{1}H NMR (300 MHz, CD_2Cl_2): δ = 7.94-7.31 (m, 40H; ph/dppe), 7.09 (s, 2H; H_5), 6.82 (s, 1H; H_7), 3.88 (s, 3H; OCH_3), 2.68 (m, 4H; CH_2/dppe), 2.08 (m, 4H, CH_2/dppe), 1.46 ppm (s, 30H; H_1); ^{13}C NMR (75 MHz, CD_2Cl_2): δ = 167.77 (s, C(O)), 137.29 (t, $^2J_{C,P}$ = 42 Hz; C_2), 134.15-127.04 (Ph), 129.03 (s, C3), 87.58 *C*$_{1'}$, 51.42 OCH_3), 30.70 (m, CH_2/dppe), 9.86 ppm (s, *C*$_1$); ^{31}P NMR (120 MHz, CD_2Cl_2): δ = 99.57 ppm (s, dppe); IR (KBr): $\bar{\upsilon}$ = 2050 (*s*) (C≡C), 1980 (*sh*) (C≡C), 1713 (*s*) (C=O), 1216 (*s*) cm^{-1} (C-O); HRMS (ESI): *m*/*z* calcd for $C_{84}H_{84}{}^{56}Fe_2O_2P_4^+$: 1360.41151 $[M]^+$; found: 1360.4123; elemental analysis calcd (%) for $C_{84}H_{84}Fe_2O_2P_4$•$0.6CH_2Cl_2$: C 71.96, H 6.08; found: C 71.99, H 6.02.

[1,3-{Cp*(dppe)Fe-C≡C-}$_2$-5-(1,4-C≡C-$C_6H_4C(O)OCH_3$)-(C_6H_3)] (**[*m*-1d]**): A Schlenk tube equipped with a reflux condenser was charged with **3d** (0.783 g, 1.77 mmol), KF (0.243 g, 4.18 mmol), KPF_6 (0.765 g, 4.18 mmol), MeOH (40 mL) and THF (4 mL), and the reagents were stired for 5 min. Then, Cp*(dppe)FeCl (2.608 g, 4.18 mmol) was added, the reaction was heated at 90 °C, and stirred for 16h. After cooling to 20 °C, the solution was treated with KOBu^t. The solvents were removed under reduced pressure, and the solid residue was extracted with dichloromethane (3 x 30 mL). The extracts were evaporated to dryness and the solid residue was washed with pentane (2 x 20 mL) and dried under vacuum. Slow diffusion of pentane into a saturated solution of **[*m*-1d]** in dichloromethane afforded red-orange crystals (0.950 g, 0.65 mmol, 37 % yield). A single crystal of this crop was selected and used for X-ray diffraction analysis. ^{1}H NMR (300 MHz, CD_2Cl_2): δ = 8.06 (d, $^3J_{H,H}$= 8.4 Hz, 2H; *H*$_{12}$), 7.90-7.38 (m, 40H; ph/dppe), 7.63 (d, $^3J_{H,H}$= 8.4 Hz, 2H; *H*$_{11}$), 6.57 (s, 1H; H_7), 6.51 (s, 2H; *H*$_5$), 3.96 (s, 3H; OCH_3), 2.72 (m, 4H; CH_2/dppe), 2.05 (m, 4H; CH_2/dppe), 1.46 ppm (s, 30H; *H*$_1$); ^{13}C NMR (75 MHz, CD_2Cl_2): δ = 166.43 (s, *C(O)*), 138.03 (t, $^2J_{C,P}$ = 38 Hz; C_2), 129.10 (s, C_3), 134.19-127.07 (*C*$_4$-*C*$_7$, *C*$_{10}$-*C*$_{13}$, *ph/dppe*), 94.42 (s, C_9), 87.70 (s, *C*$_{1'}$), 86.56 (s, C_8), 52.00 (s, OCH_3), 29.94 (m, CH_2/dppe), 9.87 ppm (s, C_1); ^{31}P NMR (120 MHz, CD_2Cl_2): δ = 101.22 ppm (s, dppe); IR (KBr): $\bar{\upsilon}$ = 2210 (*w*) (ArC≡CAr), 2106 (*w*) (Fe-C≡C), 2046 (*vs*) (FeC≡C), 1723 (*w*) (C=O), (*w*) 1270 cm^{-1} (C-O); HRMS (ESI): *m*/*z* calcd for $C_{92}H_{88}{}^{56}Fe_2O_2P_4^+$: 1460.44282 $[M]^+$; found: 1460.4433; elemental analysis calcd (%) for $C_{92}H_{88}Fe_2O_2P_4$: C 75.62, H 6.07; found: C 75.55, H 6.09.

[1,3-{Cp*(dppe)Fe-C≡C-}$_2$-5-(1,4-C≡C-$C_6H_4NO_2$)-(C_6H_3)] (**[*m*-1e]**): A Schlenk tube equipped with a reflux condenser was charged with **3e** (0.490 g, 1.18 mmol), KF (0.162 g, 2.78 mmol), KPF_6 (0.512 g, 2.78 mmol), MeOH (40 mL), THF (4 mL), and the reagents were stirred for 5 min. Then, Cp*(dppe)FeCl (1.735 g, 2.78 mmol) was added and the mixture was heated at 90 °C under stirring for 16h. After cooling to 20 °C, the solution was treated with KOBu^t. The solvents were removed under reduced pressure, and the solid residue was extracted with dichloromethane (3 x 30 mL). The extracts were evaporated to dryness and the solid residue was washed with pentane (2 x 20 mL) and dried under vacuum. Slow diffusion of pentane into a saturated solution of **[*m*-1e]** in dichloromethane afforded dark purple crystals (0.565 g, 0.39 mmol, 33% yield). A crystal of this crop was selected and used for X-ray diffraction analysis. ^{1}H NMR (300 MHz, CD_2Cl_2): δ = 8.25 (d, $^3J_{H,H}$= 8.8 Hz, 2H; *H*$_{12}$), 7.93-7.32 (m, 40H; *ph/dppe*), 7.71 (d, $^3J_{H,H}$= 8.8 Hz, 2H; *H*$_{11}$), 6.59 (s, 1H; *H*$_7$), 6.52 (s, 2H; *H*$_5$), 2.69 (m, 4H; *CH*$_2$*/dppe*), 2.07 (m, 4H; *CH*$_2$*/dppe*), 1.48 (s, 30H; *H*$_1$); ^{13}C NMR (75 MHz, CD_2Cl_2): δ = 146.65 (s, C_{13}), 137.43 (t, $^3J_{C,P}$ = 48 Hz, C_2), 134.16-123.56 (C_4-C_7, C_{10}-C_{13}, ph/dppe), 131.09 (s, C_3), 96.92 (s, C_9), 87.69 (s, *C*$_{1'}$), 85.75 (s, C_8), 30.00 (m, *CH*$_2$*/dppe*), 9.86 ppm (C_1); ^{31}P NMR (120 MHz, CD_2Cl_2): δ = 99.68 ppm (s, dppe); IR (KBr): $\bar{\upsilon}$ = 2209 (*w*) (ArC≡CAr), 2048 (*vs*) (Fe-C≡C), 1560 (*s*) (N-O), 1345 (*s*) cm^{-1} (N-O); HRMS (ESI): *m*/*z* calcd for $C_{90}H_{85}{}^{56}Fe_2NO_2P_4^+$: 1447.42241 $[M]^+$; found: 1447.4231; elemental analysis calcd (%) for $C_{90}H_{85}Fe_2NO_2P_4$•CH_2Cl_2: C 71.29, H 5.72, N 0.91; found: C 71.64, H 5.67, N 0.71.

[1,3-{Cp*(dppe)Fe-C≡C-}$_2$-5-(CH_3)-(C_6H_3)]$(PF_6)_2$ (**[*m*-1b](PF$_6$)$_2$**): A Schlenk tube was charged with compound **[*m*-1b]** (0.200 g, 0.15 mmol) and ferrocenium hexafluorophosphate (0.098 g, 0.30 mmol) before adding CH_2Cl_2 (20 mL). The mixture was stirred at 20 °C for 2h and the solvent was partially evaporated under reduced pressure to obtain 5-10 mL of solution. Then pentane was added (ca. 25 mL) to precipitate a

dark blue powder. The yellow solution which contained ferrocene was filtered off and the powder was washed with pentane (2 x 20 mL) and dried under reduced pressure to give a dark blue, almost black, powder (0.214 g, 0.1332 mmol, 87% yield). IR (KBr): $\bar{\nu}$ = 2003 (*w*) (C≡C), 1945 (*m*) (C≡C), 839 (*s*) cm^{-1} (PF$_6$); HRMS (ESI): *m*/*z* calcd for $C_{83}H_{84}{}^{56}Fe_2P_4^+$: 658.21057 [C$^+$]$^+$; found: 658.2104; m/z calcd for $C_{83}H_{84}F_6{}^{56}Fe_2P_5^+$: 1461.38587 [C$^+$,A$^-$]$^+$; found: 1461.3853; elemental analysis calcd (%) for $C_{83}H_{84}F_{12}Fe_2P_6$•1.2$CH_2Cl_2$: C 59.18, H 5.10; found: C 58.83, H 5.46.

[1,3-{Cp*(dppe)Fe-C≡C-}$_2$-5-(C(O)OCH$_3$)-(C$_6$H$_3$)](PF$_6$)$_2$ (**[*m*-1c](PF$_6$)$_2$**): Following the procedure described for **[*m*-1b](PF$_6$)$_2$**, a Schlenk tube was charged with **[*m*-1c]** (0.200 g, 0.14 mmol), ferrocenium hexafluorophosphate (0.095 g, 0.28 mmol), and 20 mL of CH_2Cl_2. After work up **[*m*-1c](PF$_6$)$_2$** was isolated (0.156 g, 0.095 mmol, 64% yield). IR (KBr, cm^{-1}): 2016 (*w*, Fe-C≡C), 1954 (*w*, Fe-C≡C), 1716 (*m*, C=O), 123é (*m*, C-O), 837 (*s,* PF$_6$); HRMS-ESI+ calc for [C]++ $C_{84}H_{84}{}^{56}Fe_2O_2P_4$, 680.20548, found, 680.2058 (0 ppm). HRMS-ESI+ calc for [C++, A-]+ $C_{84}H_{84}F_6{}^{56}Fe_2O_2P_5$, 1505.3757, found, 1505.3758 (0 ppm); elemental analysis calcd (%) for $C_{84}H_{84}F_{12}Fe_2O_2P_6$•3$CH_2Cl_2$: C, 54.56; H, 4.97. Found: C, 54.83; H, 4.76.

[1,3-{Cp*(dppe)Fe-C≡C-}$_2$-5-(1,4-C≡C-C$_6$H$_4$C(O)OCH$_3$)-(C$_6$H$_3$)](PF$_6$)$_2$ (**[*m*-1d](PF$_6$)$_2$**): Following the procedure described for **[*m*-1b](PF$_6$)$_2$**, a Schlenk tube was charged with **[*m*-1d]** (0.200 g, 0.14 mmol), ferrocenium hexafluorophosphate (0.090 g, 0.27 mmol), and 20 mL of CH_2Cl_2. After work up **[*m*-1d](PF$_6$)$_2$** was isolated (0.182 g, 0.104 mmol, 76% yield). IR (KBr): $\bar{\nu}$ = 2207 (*w*) (Ar-C≡C-Ar), 2012 (*w*) (Fe-C≡C), 1946 (*w*) (Fe-C≡C), 1713 (*m*) (C=O), 1275 (*m*) (C-O), 838 (*s*) cm^{-1} (PF$_6$); HRMS (ESI): *m*/*z* calcd for $C_{92}H_{88}{}^{56}Fe_2O_2P_4^+$: 730.22114 [C$^+$]$^+$; found: 730.2214; m/z calcd for $C_{92}H_{88}F_6{}^{56}Fe_2O_2P_5^+$: 1605.407 [C$^+$,A$^-$]$^+$; found: 1605.4072; elemental analysis calcd (%) for $C_{92}H_{88}F_{12}Fe_2O_2P_6$•$CH_2Cl_2$: C 60.83, H 5.07; found: C 60.56, H 4.94.

[1,3-{Cp*(dppe)Fe-C≡C-}$_2$-5-(1,4-C≡C-C$_6$H$_4$NO$_2$)-(C$_6$H$_3$)](PF$_6$)$_2$ (**[*m*-1e](PF$_6$)$_2$**): Following the procedure described for **[*m*-1b](PF$_6$)$_2$**, a Schlenk tube was charged with ***m*-1e** (0.100 g, 0.07 mmol), ferrocenium hexafluorophosphate (0.044 g, 0.135 mmol), and 20 mL of CH_2Cl_2. After work up **[*m*-1e](PF$_6$)$_2$** was isolated (0.076 g, 0.044 mmol, 64% yield). IR (KBr): $\bar{\nu}$ = 2212 (*w*) (Ar-C≡C-Ar), 2013 (*w*) (Fe-C≡C), 1946 (*w*) (Fe-C≡C), 1516 (*m*) (N-O), 1340 (*m*) (N-O), 839 (*s*) cm^{-1} (PF$_6$); HRMS (ESI): *m*/*z* calcd for $C_{90}H_{85}{}^{56}Fe_2NO_2P_4^+$: 723.71093 [C$^+$]$^+$; found: 723.7109; m/z calcd for $C_{90}H_{85}F_6{}^{56}Fe_2NO_2P_5^+$: 1592.3866 [C$^+$,A$^-$]$^+$; found: 1592.3865; elemental analysis calcd (%) for $C_{90}H_{85}F_{12}Fe_2NO_2P_6$•0.5$CH_2Cl_2$: C 61.04, H 4.87; found: C 60.93, H 4.93.

Mixed-Valence complexes [1,3-{Cp*(dppe)Fe-C≡C-}$_2$-5-X-(C$_6$H$_3$)](PF$_6$) (**[*m*-1b-e](PF$_6$)**). **[*m*-1b](PF$_6$):** In a Schlenk tube charged with **[*m*-1b]** (0.041 g, 0.031 mmol) and **[*m*-1b](PF$_6$)$_2$** (0.050 g, 0.031 mmol) were introduced 20 mL of CH_2Cl_2. Immediately, the color turned dark green. The mixture was stirred for 30 min and the solvent was evaporated to dryness, providing a dark green powder used for IR and NIR measurements without further treatment. **[*m*-1c](PF$_6$):** As described for **[*m*-1b](PF$_6$)**, **[*m*-1c]** (0.041 g, 0.030 mmol) and **[*m*-1c](PF$_6$)$_2$** (0.050 g, 0.030 mmol) were reacted with 20 mL of CH_2Cl_2. **[*m*-1d](PF$_6$):** Similarly, **[*m*-1d]** (0.050 g, 0.034 mmol) and **[*m*-1d](PF$_6$)$_2$** (0.060 g, 0.034 mmol) were reacted with 20 mL of CH_2Cl_2. **[*m*-1e](PF$_6$):** Similarly, **[*m*-1e]** (0.029 g, 0.020 mmol) and **[*m*-1e](PF$_6$)$_2$** (0.035 g, 0.020 mmol) were reacted with 20 mL of CH_2Cl_2.

X-ray Crystal Structure Determinations. Well-shaped single crystals of compounds **[*m*-1b]**, **[m-1d]**, and **[m-1e]**•2CH_2Cl_2 were coated in Paratone-N oil, mounted on a cryoloop and transferred to the cold gas stream of the cooling device. Intensity data were collected at T = 150(2) K on a D8 Venture Bruker AXS diffractometer equipped with a CMOS PHOTON 100 detector for **[*m*-1e]**·2CH_2Cl_2, and on a Bruker APEXII Kappa-CCD diffractometer equipped with a CCD plate detector for **[*m*-1b]** and **[*m*-1d]]**, using in all cases graphite monochromated Mo-Kα radiation (λ = 0.71073 Å), and were corrected for absorption effects using multiscanned reflections. The structures were solved by dual-space algorithm using the SHELXT program,[50] and then refined with full-matrix least-square method based on F^2 (SHELXL).[51] In compound **[*m*-1d]**, the C_6-C≡C-C_6 fragment of the bridging ligand has been modeled over two positions with refined equal occupancies of 0.50. The contribution of the disordered solvents to the calculated structure factors for **[*m*-1b]** and **[*m*-1e]** were estimated following the BYPASS algorithm,[52] implemented as the SQUEEZE option in PLATON.[53] Then, a new data set, free of solvent contribution, was used in the final refinement. For the three compounds, non-hydrogen atoms were refined with anisotropic displacement parameters. All hydrogen atoms were included in their calculated positions, assigned fixed isotropic thermal parameters and constrained to ride on their parent atoms. A summary of the details about crystal data, collection parameters and refinement are documented in Table S1, and additional crystallographic details are in the CIF files. ORTEP views were drawn using OLEX2 software.[54] CCDC reference numbers 2117753 (for **[M-1b]**), 2117755 (for **[M-1d]**) and 2117754 (for **[M-1e]**) contain the supplementary crystallographic data for this paper. These data can be obtained free of charge via http://www.ccdc.cam.ac.uk or from the CCDC, 12 Union Road, Cambridge CB2 1EZ, UK; Fax: +44 1223 336033; E-mail: deposit@ccdc.cam.ac.uk.

Acknowledgments

The MESRI (Ph.D. grant to J.L.) is acknowledged for financial support. The authors kindly thank P. Jehan (Rennes) for his assistance with HRMS experiments.

Keywords: Organoiron • Acetylides • Mixed-Valence • Molecular Structure • Charge localization

] J.-M. Lehn, *Supramolecular Chemistry - Concepts and Perspectives*, Wiley-VCH, Weinheim, **1995**.
[2] K. D. Demandis, C. M. Hartshorn, T. J. Meyer, *Chem. Rev.* **2001**, *101*, 2655.
[3] P. Chen, T. J. Meyer, *Chem. Rev.* **1998**, *98*, 1439.
[4] D. M. D'Alessandro, F. R. Keene, *Chem. Soc. Rev.* **2006**, *35*, 424.
[5] S. Záliš, R. F. Winter, W. Kaim, *Coord. Chem. Rev.* **2010**, *254*, 1383.
[6] W. Kaim, A. Klein, M. Glöckle, *Acc. Chem. Res.* **2000**, *33*, 755.
[7] P. J. Low, *Dalton Trans.* **2005**, 2821.
[8] J. P. Launay, *Coord. Chem. Rev.* **2013**, *257*, 1544.
[9] P. J. Low, *Coord. Chem. Rev.* **2013**, *257*, 1507.
[10] K. Venkatesan, O. Blacque, H. Berke, *Dalton Trans.* **2007**, 1091.
[11] K. Costuas, S. Rigaut, *Dalton Trans.* **2011**, *40*, 5643.
[12] J.-P. Launay, *polyhedron* **2015**, *86*, 151.
[13] M. Akita, T. Koike, *Dalton Trans.* **2008**, 3523.
[14] P. Safari, S. A. Moggach, P. J. Low, *Dalton Trans.* **2020**, *49*, 9835.
[15] N. Le Narvor, C. Lapinte, *Organometallics* **1995**, *14*, 634.
[16] T. Weyland, C. Lapinte, G. Frapper, M. J. Calhorda, J.-F. Halet, L. Toupet, *Organometallics* **1997**, *16*, 2024.
[17] R. Makhoul, H. Sahnoune, V. Dorcet, J.-F. Halet, J.-R. Hamon, C. Lapinte, *Organometallics* **2015**, *34*, 3314.
[18] F. Paul, C. Lapinte, *Coord. Chem. Rev.* **1998**, *178-180*, 427.
[19] J.-F. Halet, C. Lapinte, *Coord. Chem. Rev.* **2013**, *257*, 1584.
[20] T. Weyland, K. Costuas, A. Mari, J.-F. Halet, C. Lapinte, *Organometallics* **1998**, *17*, 5569.
[21] T. Weyland, K. Costuas, L. Toupet, J.-F. Halet, C. Lapinte, *Organometallics* **2000**, *19*, 4228.
[22] S. I. Ghazala, F. Paul, L. Toupet, T. Roisnel, P. Hapiot, C. Lapinte, *J. Am. Chem. Soc.* **2006**, *128*, 2463.
[23] C. Lapinte, *J. Organomet. Chem.* **2008**, *693*, 793.
[24] F. Paul, A. Bondon, G. Da Costa, F. Malvoti, S. Sinbandit, O. Cador, K. Costuas, L. Toupet, M. L. Boillot, *Inorg. Chem.* **2009**, *48*, 10608.
[25] R. C. Quardokus, Y. Lu, N. A. Wasio, C. S. Lent, F. Justaud, C. Lapinte, S. A. Kandel, *J. Am. Chem. Soc.* **2012**, *134*, 1710.
[26] Y. Lu, R. Quardokus, C. S. Lent, F. Justaud, C. Lapinte, S. A. Kandel, *J. Am. Chem. Soc.* **2010**, *132*, 13519.
[27] R. Makhoul, T. Groizard, P. Hamon, T. Roisnel, V. Dorcet, S. Kahlal, J.-F. Halet, J.-R. Hamon, C. Lapinte, *Eur. J. Inorg. Chem.* **2020**, 2624.
[28] C. S. Lent, *Science* **2000**, *288*, 1597.

[29] T. Groizard, S. Kahlal, J.-F. Halet, *inorg. Chem.* **2020**, *59*, 15772.
[30] K. Sonogashira, Y. Tohda, N. Hagihara, *Tetrahedron Lett.* **1975**, *50*, 4467.
[31] R. Denis, T. Weyland, F. Paul, C. Lapinte, *J. Organomet. Chem.* **1997**, *545-546*, 615.
[32] P. Hamon, L. Toupet, J.-R. Hamon, C. Lapinte, *Organometallics* **1996**, *15*, 10.
[33] A. J. Bard, L. R. Faulkner, *Electrochemical Methods: fundamentals and applications*, 2nd ed., John Wiley & Sons Inc., New York, **2000**.
[34] N. G. Connelly, W. E. Geiger, *Chem. Rev.* **1996**, *96*, 877.
[35] D. E. Richardson, H. Taube, *J. Am. Chem. Soc.* **1983**, *105*, 40.
[36] D. E. Richardson, H. Taube, *Coord. Chem. Rev.* **1984**, *60*, 107.
[37] F. Barrière, W. E. Geiger, *J. Am. Chem. Soc.* **2006**, *128*, 3980.
[38] M. C. B. Colbert, J. Lewis, N. J. Long, P. R. Raithby, M. Younus, A. J. P. White, D. J. Williams, N. N. Payne, L. Yellowlees, D. Beljonne, N. Chawdhury, R. H. Friend, *Organometallics* **1998**, *17*, 3034.
[39] N. J. Long, A. J. Martin, F. Fabrizi de Biani, P. Zanello, *J. Chem. Soc., Dalton Trans.* **1998**, 2017.
[40] F. Paul, L. Toupet, J.-Y. Thépot, K. Costuas, J.-F. Halet, C. Lapinte, *Organometallics* **2005**, *24*, 5464.
[41] K. Costuas, O. Cador, F. Justaud, S. Le Stang, F. Paul, A. Monari, S. Evangelisti, L. Toupet, C. Lapinte, J.-F. Halet, *Inorg. Chem.* **2011**, *50*, 12601.
[42] Y. Tanaka, J. A. Shaw-Taberlet, F. Justaud, O. Cador, T. Roisnel, M. Akita, J.-R. Hamon, C. Lapinte, *Organometallics* **2009**, *28*, 4656.
[43] E. C. Fitzgerald, A. Ladjarafi, N. J. Brown, D. Collison, K. Costuas, R. Edge, J.-F. Halet, F. Justaud, P. J. Low, H. Meghezzi, T. Roisnel, M. W. Whiteley, C. Lapinte, *Organometallics* **2011**, *30*, 4180.
[44] M. Lohan, F. Justaud, T. Roisnel, P. Ecorchard, H. Lang, C. Lapinte, *Organometallics* **2010**, *29*, 4804.
[45] M. B. Robin, P. Day, *Adv. Inorg. Chem. Radiochem.* **1968**, *10*, 247.
[46] P. Lustenberger, F. Diederich, *Helv. Chim. Acta* **2000**, *83*, 2865.
[47] X. Zhang, M. A. Ballem, M. Ahrén, A. Suska, P. Bergman, K. Uvdal, *J. Am. Chem. Soc.* **2010**, *132*, 10391.
[48] S. Takahashi, Y. Kuroyama, K. Sonogashira, N. Hagihara, *Synthesis* **1980**, 627.
[49] C. Roger, P. Hamon, L. Toupet, H. Rabaâ, J.-Y. Saillard, J.-R. Hamon, C. Lapinte, *Organometallics* **1991**, *10*, 1045.
[50] G. M. Sheldrick, *Acta Crystallogr. Sect. A* **2015**, *71*, 3.
[51] G. M. Sheldrick, *Acta Crystallogr. Sect. C* **2015**, *71*, 3.
[52] P. Van Der Sluis, A. L. Spek, *Acta Crystallogr. Sect. A* **1990**, *46*, 194.
[53] A. L. Spek, *J. Appl. Crystallogr.* **2003**, *36*, 7.
[54] O. V. Dolomanov, L. J. Bourhis, R. J. Gildea, J. A. K. Howard, H. Puschmann, *J. Appl. Crystallogr.* **2009**, *42*, 339.

10.1002/ejic.202100789

Entry for the Table of Contents

FULL PAPER

The new complexes [1,3-{Cp*(dppe)Fe-C≡C-}$_2$-5-(X)-(C_6H_3)](PF_6)$_n$ (X = CH_3, C(O)OCH_3, C≡C-4-C_6H_4-C(O)OCH_3, C≡C-4-C_6H_4-NO_2, were prepared, isolated, and characterized for *n* = 0-2. The analyses by CV, IR and NIR spectroscopies establish that the electronic properties are sensed by the metal centers through eleven bonds.

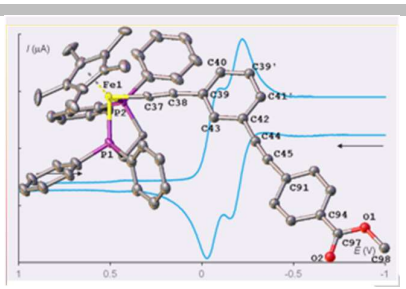

Molecular Electronics

Joseph Lepont, Thierry Roisnel, Jean-René Hamon, and Claude Lapinte**

Page No. – Page No.

1,3-Diethynyl-5-(X)-benzene-Bridged [Cp*(dppe)Fe]n+ Units: Effect of Substituents on the Metal-Metal Interactions